

Radiation Research Institute, Hyogo, Japan with approval from the Animal Experiment Review Committee in accordance with the guidelines of the Physiological Society of Japan, as previously described (**Figure 4**).³ In brief, under sodium pentobarbital anesthesia (50 mg/kg i.p.), examined rats were intubated and artificially ventilated (Shinano, Tokyo, Japan; 40% oxygen), then the right carotid artery was cannulated with a radiopaque 20-gauge BD Angiocath catheter (Becton Dickinson, Inc., Sandy, Utah, USA), placing the tip at the entrance of the aortic valve. Each rat was then placed in line with the horizontal X-ray beam and SATICON detector system (Hitachi Denshi Techno-system, Ltd., Tokyo, Japan and Hamamatsu Photonics, Shizuoka, Japan). Iodinated contrast medium (Iomeron 350; Bracco-Eisai Co. Ltd, Tokyo, Japan) was injected intrarterially as a bolus (0.3-0.5 ml at 0.4 ml/s) into the aorta using a clinical autoinjector (Nemoto Kyorindo, Tokyo, Japan) at the start of image recording scanning. At least 10 minutes was allowed for renal clearance of the contrast between imaging scans. Following a baseline recording, an endothelium-dependent vasodilatory response was recorded as an angiogram series at the end of a 5-minute infusion of acetylcholine (5 µg/kg/min). A third image series was recorded after a 5-minute infusion of dobutamine hydrochloride (8 µg/kg/min) to assess the ability to maintain perfusion of the infarcted region during increased heart work.

Assessment of Vessel ID during Synchrotron Angiography

Quantitative analysis of vessel internal diameter (ID) was based on measurements from the middle of discrete vessel segments in individual cine-radiogram frames using Image-J (v1.41, NIH, Bethesda, USA) for individual rats during each treatment period. Arterial vessels were categorized according to their branching order.³ The results for vessel ID in each rat during drug infusions are expressed as percentage changes from baseline (Δ), to account for

differences in absolute baseline vessel ID among the groups.

Quantification of Segmental Vasoconstrictions during Synchrotron Angiography

The relative change in vessel caliber in response to vasoactive agents gives no indication of vessel number with calibers less than the individual's mean change. Therefore, the number of abnormal vasoconstrictions during treatment periods was quantified. Localized segmental vasoconstrictions were considered to be present when a vessel segment showed an ID constriction of >5% of baseline vessel ID value.^{3,4}

PET measurements and data analysis

To evaluate the effects of each treatment on global and regional myocardial blood flow (MBF) and coronary flow reserve (CFR), ¹³N-ammonia PET measurements were serially performed 1 day before and 3 weeks after treatment (control: n=5, combined: n=8, cell-sheet: n=7, OM: n=7) (**Figure 5**). Rats were anesthetized with 2% isoflurane plus 100% oxygen and a cannula was inserted into the tail vein. PET data were acquired using a small animal PET device (Inveon PET/CT system, Siemens). Dynamic 10-minute PET measurements were started with an administration of ¹³N-NH₃ over 20 seconds (approximately 20 and 80 MBq for the rest and stress study, respectively).⁵ The stress study was performed 5 minutes after bolus injection of CGS-21680 (5 µg/kg), a selective adenosine A_{2A} agonist that induced coronary vasodilatation and increases in the MBF.

The PET data were reconstructed into 23 frames (12 fr × 5 s, 6 fr × 10 s, 4 fr × 30 s, 1 fr × 360 s) using the 3-dimensional ordered subset expectation maximization method followed by maximum a posteriori (3D-OSEM/MAP). Regions of interest were semi-automatically placed on the left ventricle myocardium and blood pooled inside the left and right ventricle, with

reference to the summed PET and CT images. MBF was calculated using the one-tissue compartment model developed by DeGrado et al. with PMOD software.⁶ Global and regional MBF (basal, mid, apical segments) were used for the evaluations.⁷ CFR was expressed as the ratio of MBF during stress to MBF at rest. Change in CFR was evaluated as the ratio of post-treatment to pre-treatment CFR. Normal male SD rats (n=6, 10-11 weeks old, BW: 369-429 g) were used for the validation study for quantitative PET measurements with a stress agent.

Assessment of Cardiac Function

The cardiac function was evaluated by echocardiography 2 and 4 weeks after each treatment (n=11 for each group) (**Figure 6**). Baseline measurements were made before each treatment. Transthoracic echocardiography was performed with using a SONOS 5500 (Philips Electronics, Tokyo, Japan) equipped with a 12-MHz annular array transducer under general anaesthesia induced and maintained by inhalation of isoflurane (2%, 0.2 mL/min) as mentioned above (**Figure 1**). The hearts were imaged in short-axis 2D views at the level of the papillary muscles, and the LV end-systolic and end-diastolic dimensions were determined. LV ejection fraction was calculated by Pombo's method.

LV pressure-volume loop analysis with cardiac catheterization was performed for each group as previously described.¹ In brief, a median sternotomy was performed and the LV apex was carefully dissected to minimize hemorrhaging. A MicroTip catheter transducer (SPR-671; Millar Instruments, Inc, Houston, Tex) and conductance catheter (Unique Medical Co, Tokyo, Japan) were then placed longitudinally into the left ventricle from the apex. LV pressure-volume relationships were determined by transiently compressing the inferior vena cava.

Exercise Tolerance

Eleven rats in each group were acclimated to a rodent activity wheel (MULTI-FUNCTIONAL ACTIVITY WHEEL, MK-770M, Muromachi, Tokyo, Japan) by running daily for 5 days. During the acclimation period, the round speed was increased from 5 to 10 rpm, with the exercise duration maintained at 20 minutes. On the day of tolerance testing, animals were placed on the activity wheel at round speeds of 4 or 8 rpm and allowed to exercise until fatigue. Fatigue was defined as the point at which the animal failed to keep pace with the activity wheel despite constant physical prodding for 1 minute. Running distance was used as an index of maximal capacity for exercise.

Communication Between Pedicle Omentum and Native Coronary Artery

Communication between the coronary arteries and branches of the gastroepiploic artery in the OM specimens was evaluated using 3 different methods in a different series of OM-only and combined group (n=12 for each group) (**Figure 7**).

Aortic Root Angiography using Barium Sulfate

We performed a postmortem angiography examination from the aortic root to verify antegrade flow from the OM into the heart (n=4 for each). In brief, a catheter with an internal diameter of 0.89 mm (COVIDIEN Ltd, Tokyo, Japan) was inserted from the right carotid artery into the aortic root, followed by systemic heparinization (1000 IU heparin). The rats were euthanized with an overdose of pentobarbital, then an incision was made in the right jugular vein and lactated Ringer's solution was manually perfused through the cannula for 5 minutes. Approximately 3 mL of a solution consisting of 70% weight/volume barium sulfate

suspended in 7% gelatin was then injected in a retrograde manner via the catheter using a programmed syringe pump. Angiograms were obtained with a angiographic system (MFX-80HK, Hitex) consisting of an open type 1- μ m microfocus X ray source (L9191, Hamamatsu Photonics) and a 50/100 mm (2³/₄") dual mode X-ray image intensifier (E5877JCD1-2N, Toshiba) set at 60 kV and 60 μ A.

Selective India Ink Perfusion via Celiac Artery

Next, we selectively injected India ink into the celiac artery to visually and histologically confirm vessel communication between the pedicle OM and native coronary artery (n=4 for each). The catheter was inserted via the abdominal aorta and its tip placed near the celiac artery, followed by systemic heparinization. The chest was reopened to expose the wrapped heart, taking care to avoid injuring the OM. The heart was harvested after perfusion fixation of the vasculature, as described above. We ligated the abdominal aorta just proximal from the tip of the catheter in advance and selectively injected India ink via the celiac artery into the heart, and then performed histological analysis.

Selective Perfusion via Aortic Root and Celiac Artery Using Two Different MICROFIL Colors

A catheter was inserted from the right carotid artery into the aortic root and another was inserted from the abdominal aorta into the celiac artery, followed by systemic heparinization (1000 IU heparin). After perfusion fixation, we ligated the abdominal aorta just proximal from the tip of the catheter. Approximately 3 mL of 2 different colors of MICROFIL solution (MICROFIL Silicone Rubber Injection Compounds, Flow Tech, Inc.) was injected in an antegrade manner into the celiac arterial trunk (MV-120 Blue) and a retrograde manner from

the aortic root into the coronary artery (MV-117 Orange). The solution was allowed to solidify for more than 30 minutes. The heart and OM were removed en bloc, and placed in 10% neutral buffered formalin for several days. The tissue was then cleared using sequential 24-hour incubations in 25% ethanol, 50% ethanol, 75% ethanol, 95% ethanol, 100% ethanol, and methylsalicylate, according to the manufacturer's instructions. Evidence of vessel communication between the native coronary artery and OM-flap was photographed in multiple planes using an Olympus DP70 camera attached to an Olympus SZX 12 stereo microscope (Olympus, Tokyo, Japan).

Creation of Surgically Joined Parabiotic Pairs Model

To further confirm whether the OM- and host myocardium-derived endothelial cells migrated toward the cell-sheet, we established two types of parabiotic pair models (n=4 for each) (**Figure 8**). To determine whether OM-derived endothelial cells migrated toward the cell-sheet, the parabiotic pairs model were established by producing wild-type MI model rats (recipient) to receive transplantation of wild-type oriented cell-sheets which was labeled with Cell Tracker TM Orange CMTMR (Invitrogen, Oregon, USA), followed by coverage with a pedicle OM derived from a transgenic ubiquitously expressing GFP rat (donor) and then surgically joining them. Similarly, to determine whether host myocardium-derived endothelial cells migrated toward the cell-sheet, we also established another parabiotic pairs model by producing GFP-transgenic MI model rats (recipient) to receive transplantation of wild-type oriented cell-sheets which was labeled with Cell Tracker TM Orange CMTMR, followed by coverage with a pedicle OM derived from a wild-type rat (donor) and then surgically joining them.

Parabiotic pair rats were anaesthetized by inhalation of isoflurane (2%, 0.2 mL/min) and

maintained for 72 hours under mechanical ventilation with a continuous infusion of 5% glucose (0.3 ml/h), then subjected to histological analyses.

In vitro Migration assay

To investigate cell migration in response to skeletal myoblast cells cultured in conditioned medium, a modified Boyden chamber migration assay was performed using an HTS FluoroBlok™ Multiwell Insert System (BD Falcon, NJ, USA) containing filters with a pore size of 8 µm. Briefly, human umbilical vein endothelial cells (HUVECs) (purchased from Lonza) were grown in EGM-2 culture medium (Lonza, Walkersville, USA). To visualize them, HUVECs were stained in advance with Cell Tracker™ Orange CMTMR (Invitrogen, Oregon, USA). A suspension of 5×10^4 HUVECs in HUVEC-cultured medium (350 µm) was applied to each upper chamber. The lower chamber was filled with 1.0 ml of concentrated skeletal myoblasts-cultured supernatant composed of DMEM with 20% fetal bovine serum (100% conditioned medium), 10-fold diluted conditioned medium (10% conditioned medium) or DMEM, and 20% fetal bovine serum (control group). After incubation at 37°C for 2 hours, the number of migrated cells was counted in 15 randomly chosen fields under 100×magnification using fluorescence microscopy (BIOREVO BZ-9000, KEYENCE, Osaka, Japan). Two replicate samples were used in each experiment, which were performed at least twice. Migrating cells were analyzed using a light microscope and reported as numbers of migrating cells per mm².

Statistical analysis

Data are expressed as the mean ± SEM unless otherwise stated. Student's t test (2 tailed) was used to compare 2 groups of independent samples. One-way and two-way ANOVA with

Bonferroni correction for repeated measures were performed to assess within and between group differences following the treatments. Following ANOVA, between group comparisons were made using a Student's t-test (2-tailed). Multiplicity in pairwise comparisons was corrected by the Bonferroni procedure. The Statistical Package Software System (SPSS v15, SPSS Inc, Chicago, USA) and JMP 9.0 (SAS Institute Inc, Cary, NC) were used for all analyses, with P values <0.05 deemed to indicate significance.

References

1. Sekiya N, Matsumiya G, Miyagawa S, Saito A, Shimizu T, Okano T, Kawaguchi N, Matsuura N, Sawa Y. Layered transplantation of myoblast sheets attenuates adverse cardiac remodeling of the infarcted heart. *J Thorac Cardiovasc Surg* 2009;**138**:985-993.
2. Mancuso MR, Davis R, Norberg SM, O'Brien S, Sennino B, Nakahara T, Yao VJ, Inai T, Brooks P, Freimark B, Shalinsky DR, Hu-Lowe DD, McDonald DM. Rapid vascular regrowth in tumors after reversal of VEGF inhibition. *J Clin Invest* 2006;**116**:2610-2621.
3. Jenkins MJ, Edgley AJ, Sonobe T, Umetani K, Schwenke DO, Fujii Y, Brown RD, Kelly DJ, Shirai M, Pearson JT. Dynamic synchrotron imaging of diabetic rat coronary microcirculation in vivo. *Arterioscler Thromb Vasc Biol* 2012;**32**:370-377.
4. Ludmer PL, Selwyn AP, Shook TL, Wayne RR, Mudge GH, Alexander RW, Ganz P. Paradoxical vasoconstriction induced by acetylcholine in atherosclerotic coronary arteries. *N Engl J Med* 1986;**315**:1046-1051
5. Croteau E, Bénard F, Bentourkia M, Rousseau J, Paquette M, Lecomte R. Quantitative myocardial perfusion and coronary reserve in rats with ¹³N-ammonia and small animal PET: impact of anesthesia and pharmacologic stress agents. *J Nucl Med* 2004;**45**:1924-1930.
6. DeGrado TR, Hanson MW, Turkington TG, DeLong DM, Brezinski DA, Vallée JP, Hedlund LW, Zhang J, Cobb F, Sullivan MJ, Coleman RE. Estimation of myocardial blood flow for longitudinal studies with ¹³N-labeled ammonia and positron emission tomography. *Med J Nucl Cardiol* 1996;**3**:494-507.
7. Cerqueira MD, Weissman NJ, Dilsizian V, Jacobs AK, Kaul S, Laskey WK, Pennell DJ, Rumberger JA, Ryan T, Verani MS; American Heart Association Writing Group on Myocardial Segmentation and Registration for Cardiac Imaging. Standardized myocardial

Kainuma S. et al. Cell-sheets Therapy Combined with Omentum flap - 16 -

segmentation and nomenclature for tomographic imaging of the heart. A statement for healthcare professionals from the Cardiac Imaging Committee of the Council on Clinical Cardiology of the American Heart Association. *Circulation* 2002;**29**;105:539-542.



Targeted Delivery of Adipocytokines Into the Heart by Induced Adipocyte Cell-Sheet Transplantation Yields Immune Tolerance and Functional Recovery in Autoimmune-Associated Myocarditis in Rats

Sokichi Kamata, MD, PhD; Shigeru Miyagawa, MD, PhD; Satsuki Fukushima, MD, PhD;
Yukiko Imanishi, PhD; Atsuhiko Saito, PhD; Norikazu Maeda, MD, PhD;
Ichiro Shimomura, MD, PhD; Yoshiki Sawa, MD, PhD

Background: Clinical prognosis is critically poor in fulminant myocarditis, while its initiation or progression is fated, in part, by T cell-mediated autoimmunity. Adiponectin (APN) and associated adipokines were shown to be immune tolerance inducers, although the clinically relevant delivery method into target pathologies is under debate. Whether the cell sheet-based delivery system of adipokines might induce immune tolerance and functional recovery in experimental autoimmune myocarditis (EAM) was tested.

Methods and Results: Scaffold-free-induced adipocyte cell-sheet (iACS) was generated by differentiating adipose tissue-derived syngeneic stromal vascular-fraction cells into adipocytes on temperature-responsive dishes. Rats with EAM underwent iACS implantation or sham operation. Supernatants of iACS contained a high level of APN and hepatocyte growth factor (HGF), and reduced proliferation of CD4-positive T cells in vitro. Immunohistolabelling showed that the iACS implantation elevated the levels of APN and HGF in the myocardium compared to the sham operation, which attenuated the immunological response by inhibiting CD68-positive macrophages and CD4-positive T-cells and activating Foxp3-positive regulatory T cells. Consequently, left ventricular ejection fraction was significantly greater after the iACS implantation than after the sham operation, in association with less collagen accumulation.

Conclusions: The targeted delivery of adipokines using tissue-engineered iACS ameliorated cardiac performance of the EAM rat model via effector T cell suppression and induction of immune tolerance. These findings might suggest a potential of this tissue-engineered drug delivery system in treating fulminant myocarditis in the clinical setting. (*Circ J* 2015; **79**: 169–179)

Key Words: Adiponectin; Inflammation; Myocarditis; Transplantation

Fulminant myocarditis often follows a rapidly deteriorating course, leading to severe cardiac dysfunction. Efficacy of fast-track immunoglobulin and steroid therapies has been reported,¹ but these treatments are not fully established. Although the pathogenesis of fulminant myocarditis is not fully understood, an autoimmune response against myocardial components has been suggested to play an important role in its progression, consequently leading to end-stage heart failure.^{1,2} Interferon (IFN) γ -producing T helper (Th)1 cells and interleukin (IL)17-producing Th17 cells are reported to be key regulators of the autoimmune response, as they ac-

tivate macrophages in the cardiac tissues to trigger inflammation and inhibit regulatory T cells.^{2,3} Strategies for ameliorating the immune response and/or augmenting immune tolerance are therefore under development for treating fulminant myocarditis.

Editorial p51

Fat tissue functions as a type of endocrine organ by secreting its produced cytokines and adipokines, which have pro-inflammatory and anti-inflammatory activities. Adiponectin

Received July 31, 2014; revised manuscript received September 13, 2014; accepted September 24, 2014; released online November 5, 2014 Time for primary review: 19 days

Department of Cardiovascular Surgery (S.K., S.M., S.F., Y.I., A.S., Y.S.), Department of Metabolic Medicine (N.M., I.S.), Osaka University Graduate School of Medicine, Suita, Japan

Mailing address: Yoshiki Sawa, MD, PhD, Department of Cardiovascular Surgery, Osaka University Graduate School of Medicine, 2-2 Yamadaoka, Suita 565-0871, Japan. E-mail: sawa-p@surg1.med.osaka-u.ac.jp

ISSN-1346-9843 doi:10.1253/circj.CJ-14-0840

All rights are reserved to the Japanese Circulation Society. For permissions, please e-mail: cj@j-circ.or.jp

(APN) is an adipokine with strong anti-inflammatory properties and has been suggested to play a protective role in the acute phase of myocarditis in humans.^{4,5} Importantly, it has been known that APN is downregulated in a variety of clinical conditions or critical illnesses, such as obesity, type 2 diabetes, and coronary artery disease.⁶ In addition, hepatocyte growth factor (HGF), another known anti-inflammatory adipokine, was reported to induce immune tolerance and functional recovery by use of an *in vivo* transfection technique in experimental autoimmune myocarditis (EAM).^{7,8} However, no clinically relevant method for the efficient delivery of APN or HGF into the heart has been well established for treating fulminant myocarditis.

We previously developed the epicardial transplantation of scaffold-free-induced adipocyte cell-sheet (iACS) method, and recently showed that iACS can constitutively deliver a variety of cardioprotective factors, including APN and HGF, to the heart in mice subjected to acute myocardial infarction.⁹ Importantly, iACS is generated from adipose tissue-derived stromal vascular fraction (SVF) cells that are isolated from the subcutaneous fat tissue without gene modification, which is promising for the potential use of this method in clinical settings.

We hypothesized that iACS transplantation into the heart might induce immune tolerance and functional recovery in autoimmune-associated myocarditis. Here we examined the biological and functional effects of this method as a drug-delivery system using an EAM rat model. Immunoinhibitory effects of pivotal paracrine factors, such as APN and HGF, on dendritic and effector T cells were also analyzed *in vivo* and *in vitro*. In addition, we generated a non-differentiating SVF cell-sheet (SVFCS) and showed that both the iACS and SVFCS produce a similarly great amount of anti-inflammatory adipokines, including HGF; however, differentiated iACS but not SVFCS was able to secrete a large amount of APN. Therefore, for the purpose of examining the additional effect of APN on EAM, we compared the therapeutic effects of iACS implantation with those of SVFCS implantation.

Methods

Animals

All animal studies were carried out under approval of the institutional ethics committee. This investigation conforms to the Principles of Laboratory Animal Care formulated by the National Society for Medical Research and the Guide for the Care and Use of Laboratory Animals (US National Institutes of Health Publication No. 85-23, revised 1996).

Preparation of SVFCS and iACS

Each iACS was prepared as previously described.⁹ Briefly, SVF cells isolated from inguinal adipose tissue were cultured on 35-mm thermo-responsive dishes (CellSeed, Tokyo, Japan), at 2×10^6 cells per dish, to generate each scaffold-free SVFCS. Each iACS was generated by adding 10 mg/ml insulin, 2 mmol/L dexamethasone, 5 mmol/L pioglitazone, and 125 mmol/L isobutylmethylxanthine (Sigma-Aldrich, St Louis, MO, USA) to the SVFCS for 2 days. The medium was then refreshed and the cultures incubated for 5 more days at 37°C. The iACS spontaneously detached from the surface when placed in a 20°C refrigerator.

Generation of the Rat Myocarditis Model and Cell-Sheet Transplantation

Purified porcine cardiac myosin (Sigma-Aldrich) was dis-

solved in 0.01 mol/L phosphate-buffered saline and emulsified with an equal volume of complete Freund's adjuvant (Difco Laboratories, Detroit, MI, USA). On days 0 and 7, 0.2 ml of the emulsion, which yielded an immunizing dose of 1.0 mg cardiac myosin per rat, was injected subcutaneously into the footpad of male Lewis rats (7 weeks old, 200–250 g).² Following the second injection, the rats were randomly assigned to 3 groups and subjected to a thoracotomy and: (1) a sham operation (Sham group; n=58) or transplantation onto the anterior surface of the heart of; (2) 3-layered SVFCS (SVFCS group; n=54); or (3) 3-layered iACS (iACS group; n=58).

Echocardiography and Conductance Catheter

Serial transthoracic echocardiography was performed under inhaled anesthesia with isoflurane (1.5%, 1 L/min; Mylan, Pittsburgh, PA, USA). Two-dimensional short-axis images at the basal, mid, and apical levels were acquired to calculate the left ventricular (LV) ejection fraction (EF) and regional wall motion index (RWMI).¹⁰

Pressure-volume (P-V) cardiac catheterization was performed after median sternotomy, by inserting a conductance catheter (Unique Medical, Tokyo, Japan) and a Micro Tip catheter transducer (SPR-671; Millar Instrument, Houston, TX, USA) into the LV cavity. The P-V loop data under stable hemodynamics or inferior vena cava occlusion were analyzed with Integral 3 software (Unique Medical).

CD4-Positive T-Cell Proliferation Assay

CD4-positive T cells and antigen-presenting dendritic cells were isolated from the spleen of EAM and normal rats, respectively, using magnetic-bead systems (Miltenyi Biotec, Bergish Gladbach, Germany). The isolated CD4-positive T cells and antigen-presenting dendritic cells were co-cultured in RPMI 1640 (Gibco, Grand Island, NY, USA) and 10% fetal bovine serum (FBS), supplemented with iACS supernatant, recombinant APN (Adipo Bioscience, CA, USA), or recombinant HGF (Institute of Immunology, Tokyo, Japan) for 5 days. Subsequently, 50 µg/ml purified porcine heart myosin was added, and T-cell proliferation was estimated using the Cell Counting Kit-8 (Dojindo, Kumamoto, Japan).⁸

Histology

Myocarditis severity was graded on hematoxylin and eosin (H&E)-stained whole sections (0, no inflammatory infiltrates; 1, small foci of inflammatory cells; 2, larger foci <100 inflammatory cells; 3, more than 10% of a cross-section involved; and 4, more than 30% of a cross-section involved).¹¹ The CD68-, CD4-, or CD4/Foxp3-positive cells were counted in 5 random fields (magnification: $\times 600$) to assess the infiltration of macrophages, CD4-positive T cells, or Foxp3-positive regulatory T cells, respectively.⁸

Statistical Analysis

Values are given as the mean \pm SD. All analyses were performed using SPSS 11.0J for Windows (SPSS, Chicago, IL, USA) and the R program.

Detailed methods are presented in Supplementary File 1.⁹

Results

Characterization of SVFCS and iACS *In Vitro*

The characteristics and fundamental behavior of the SVFCS and iACS were compared histologically and biochemically *in vitro*. The cells in the SVFCS were confluent and spindle-shaped. The cells in iACS were similar but many contained a

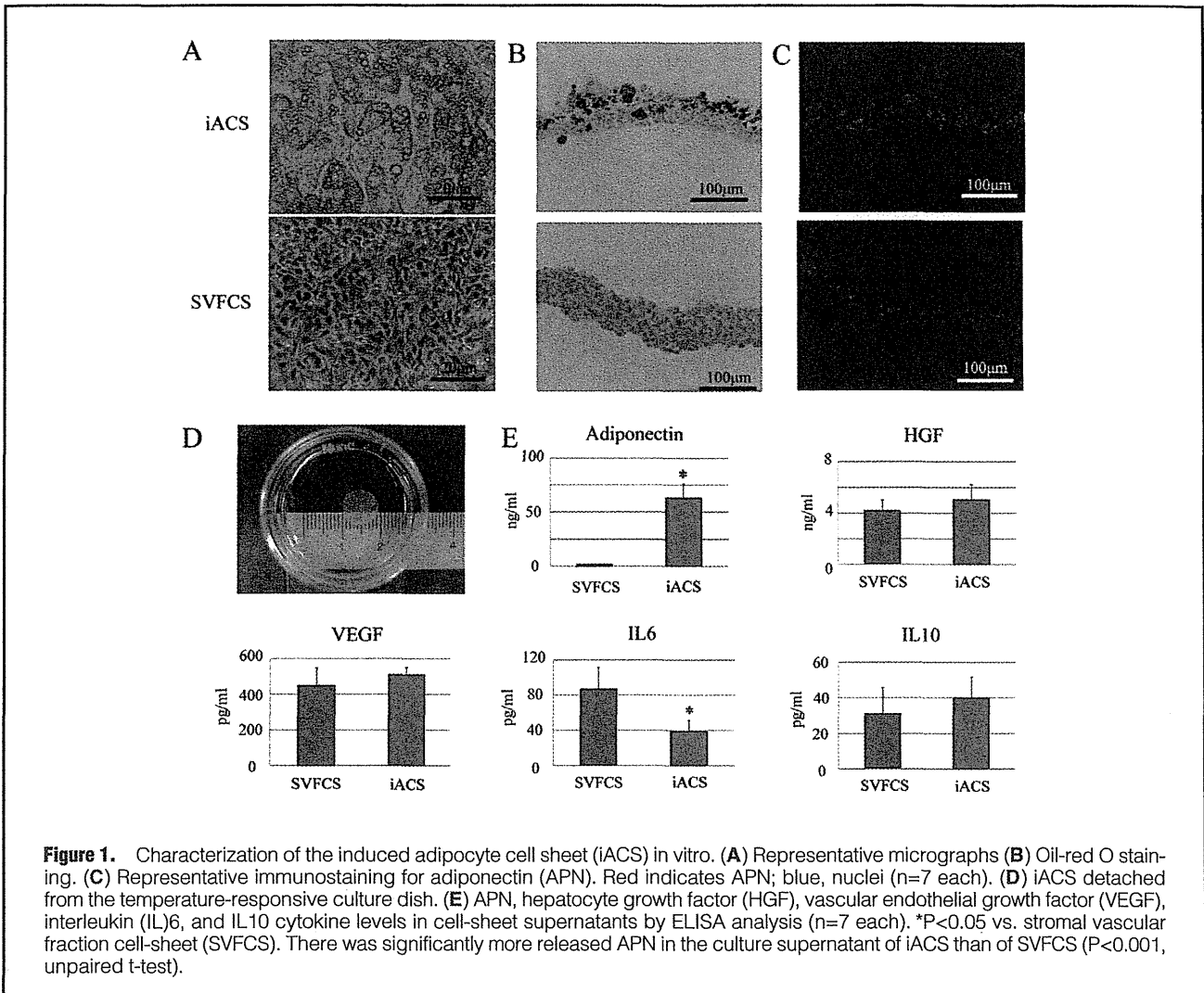


Figure 1. Characterization of the induced adipocyte cell sheet (iACS) in vitro. (A) Representative micrographs (B) Oil-red O staining. (C) Representative immunostaining for adiponectin (APN). Red indicates APN; blue, nuclei (n=7 each). (D) iACS detached from the temperature-responsive culture dish. (E) APN, hepatocyte growth factor (HGF), vascular endothelial growth factor (VEGF), interleukin (IL)6, and IL10 cytokine levels in cell-sheet supernatants by ELISA analysis (n=7 each). *P<0.05 vs. stromal vascular fraction cell-sheet (SVFCS). There was significantly more released APN in the culture supernatant of iACS than of SVFCS (P<0.001, unpaired t-test).

number of small cytoplasmic vesicles (Figure 1A) that stained positive with oil-red O, indicating that the vesicles were fat droplets. Only approximately half the SVF cells had differentiated into adipocytes (Figure 1B). Each iACS was approximately 9 mm in diameter and 140- μ m thick (Figure 1D). Immunohistolabeling revealed that APN was markedly upregulated in the cytoplasm of mature adipocytes in the iACS, but not in the undifferentiated SVF cells in the SVFCS (Figure 1C). The amount of extracellularly released APN in vitro was significantly and markedly greater in the culture supernatant of the iACS than in that of the SVFCS (P<0.001), as assessed by enzyme-linked immunosorbent assay (ELISA) (Figure 1E). The levels of HGF, vascular endothelial growth factor (VEGF) and anti-inflammatory IL10 were not significantly different between the SVFCS and the iACS, whereas the level of pro-inflammatory IL6 in the iACS culture supernatant was significantly lower (P=0.001).

Inhibition of Antigen-Specific CD4-Positive T-Cell Proliferation by iACS In Vitro

We first examined the expression of 2 different APN receptors (AdipoR1 and AdipoR2) in CD4-positive T cells, CD8-positive T cells and dendritic cells. Using quantitative real-time PCR, we detected similar levels of 2 genes in these 3 cell types

(Figure 2A).

Next, the effects of iACS transplantation on CD4-positive T-cell-related immunity in the EAM rats were assessed by an antigen-specific T-cell proliferation assay in vitro.

The addition of porcine myosin significantly and markedly increased the proliferation of CD4-positive T cells that were isolated from the spleen of the EAM rats (Figure 2B). The addition of recombinant APN and HGF at more than 30 ng/ml and 2 ng/ml, respectively, significantly suppressed the antigen-induced CD4-positive T-cell proliferation (Figure S1). The proliferation was diminished significantly more by the addition of an iACS supernatant, compared with 60 ng/ml APN or 5 ng/ml HGF, which were the average amounts released by iACS in vitro (P<0.001 for Myosin (+) vs. APN (60 ng/ml) and HGF (5 ng/ml vs. iACS supernatant). VEGF addition did not have any effect on T-cell proliferation (data not shown). ELISA analysis of the supernatant after incubating the antigen-induced CD4-positive T cells with a specific antigen revealed that adding recombinant APN (60 ng/ml), recombinant HGF (5 ng/ml) or iACS supernatant significantly diminished the release of IFN γ , IL17 and IL6 from the cells (Figures 2C–E).

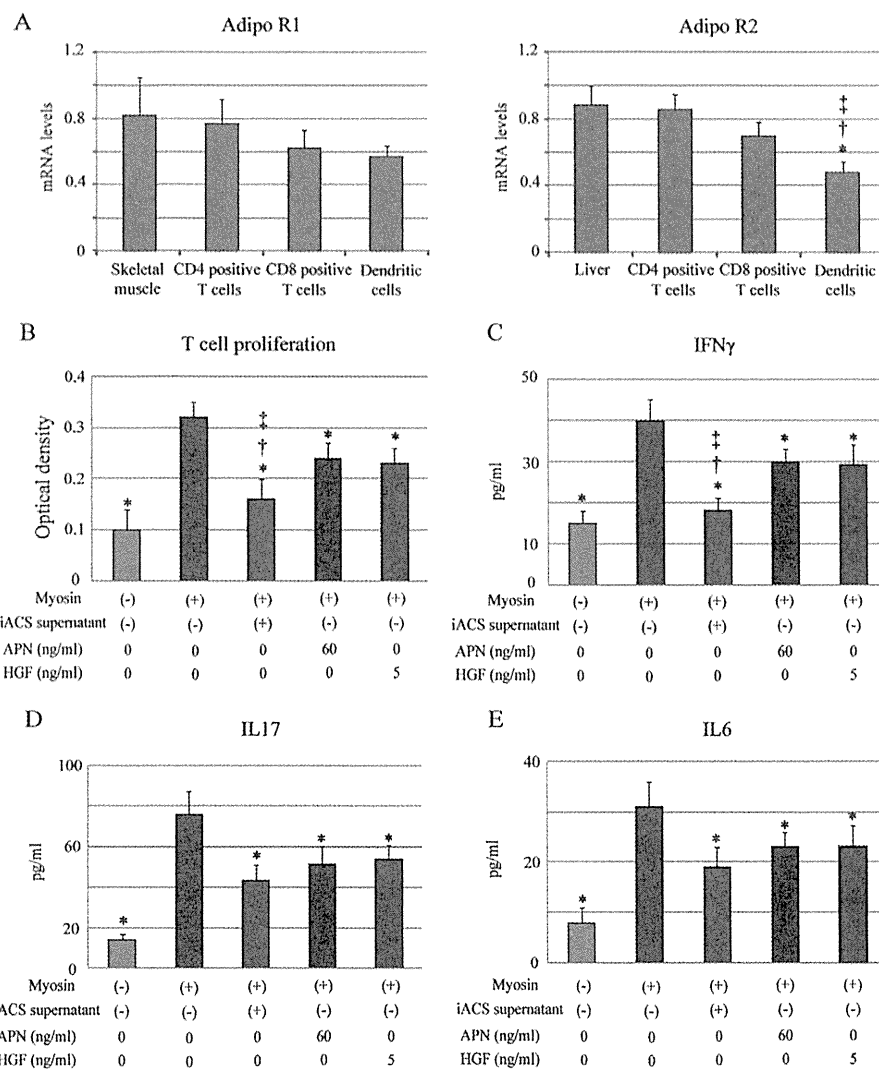


Figure 2. Expression of adiponectin (APN) receptors and CD4-positive T-cell proliferation assay. (A) mRNA levels of 2 different APN receptors (AdipoR1 and AdipoR2) in CD4-positive T cells, CD8-positive T cells and dendritic cells ($n=7$ each, ANOVA). * $P<0.05$ vs. Liver, † $P<0.05$ vs. CD4 positive T cells, ‡ $P<0.05$ vs. CD8 positive T cells. All mRNA levels are normalized to GAPDH. (B–E) Addition of induced adipocyte cell-sheet (iACS) supernatant, recombinant APN (60ng/ml) or hepatocyte growth factor (HGF) (5 ng/ml) significantly suppressed the CD4-positive T-cell proliferation (IFN γ ($P<0.001$), interleukin (IL)17 ($P<0.001$) and IL6 ($P<0.001$) ($n=7$ each, ANOVA). * $P<0.05$ vs. Myosin (+), † $P<0.05$ vs. APN (60ng/ml), ‡ $P<0.05$ vs. HGF (5 ng/ml).

Delivery of APN, HGF and VEGF Into EAM Rat Heart by iACS Transplantation

The expression of APN, HGF and VEGF in the EAM rat heart after treatment was assessed by immunohistolabeling and ELISA. Most of the green fluorescent protein (GFP)-positive transplanted cells on day 21 in both the SVFCS and iACS groups remained on the surface of the heart (Figures 3B,C), and the number in both engrafted cell sheets gradually decreased from day 8 to day 42 (SVFCS: $P=0.026$, iACS: $P=0.045$; Figure 3J). Relatively small amounts of APN were detected at the inflamed interstitium and perivascular area in the Sham and SVFCS groups on day 21 (Figures 3A,B). In the iACS group, APN expression was higher at the interstitium near the inflammatory cells and the perivascular area,

especially in the epicardium near the transplanted iACS.

ELISA showed that the cardiac expression of APN in the inflamed area gradually increased over 42 days in the Sham and SVFCS groups, whereas the iACS transplantation significantly and markedly increased the APN expression compared to the other groups for 21 days; thereafter, high APN expression was maintained through the 42 days of the experiment (APN on day 21: $P=0.007$ for iACS vs. SVFCS and Sham; Figure 3G). Both HGF and VEGF were expressed in the inflamed area, but not in the non-inflamed area, on day 21 as assessed by immunohistolabeling (data not shown); the expression levels of HGF and VEGF on days 21 and 42 were similarly greater in the SVFCS and iACS groups than in the Sham group ([HGF on day 21: $P=0.001$ for iACS and SVFCS

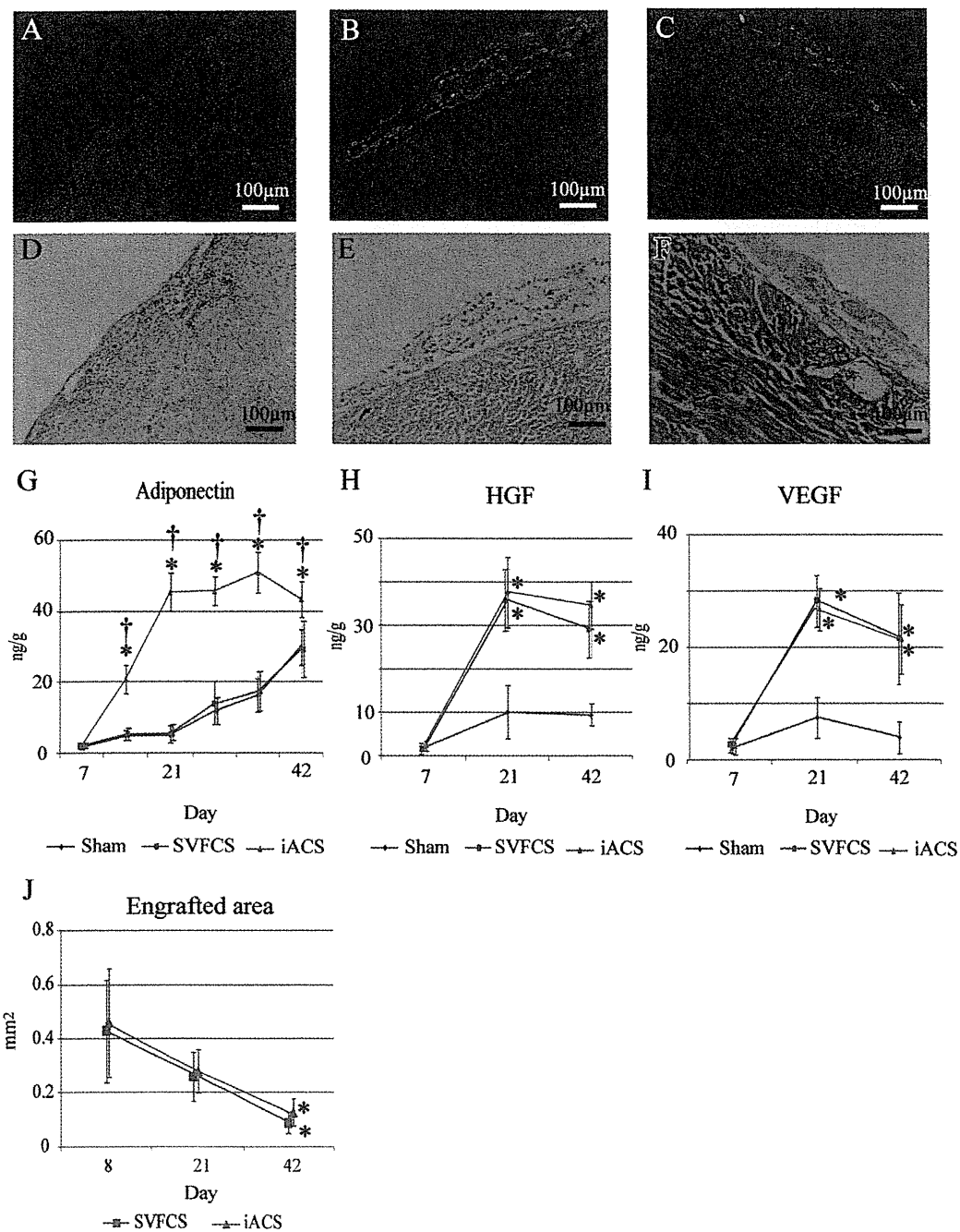


Figure 3. Delivery of cardioprotective factors to the experimental autoimmune myocarditis (EAM) rat heart by induced adipocyte cell-sheet (iACS) transplantation in vivo. (A–C) Representative immunostaining for adiponectin (APN) 14 days after the Sham operation (A), or green fluorescent protein (GFP)-positive stromal vascular-fraction cell-sheet (SVFCS) (B) and iACS (C) transplantation, respectively. Red, APN; blue, nuclei. (D–F) Hematoxylin and eosin staining of a serial section from the sample in (A), (B) and (C), respectively. (G–I) Cardiac expression of APN (G), hepatocyte growth factor (HGF) (H), and vascular endothelial growth factor (VEGF) (I) over time by ELISA (APN: Sham, n=7; SVFCS, n=6; iACS, n=7) (HGF and VEGF: Sham, n=6; SVFCS, n=5; iACS, n=7). *P<0.05 vs. Sham, †P<0.05 vs. SVFCS. (J), Quantification of the engrafted GFP-positive cell-sheet area in the iACS and SVFCS groups (n=4 each). *P<0.05 vs. day8.

vs. Sham] [VEGF on day 21: P<0.001 for iACS and SVFCS vs. Sham]) (Figures 3H,I).

Induced ACS Transplantation Ameliorates Autoimmune Myocarditis in Rats

The severity of myocarditis in the EAM rats on day 21 was assessed and scored using H&E-stained heart sections (n=12

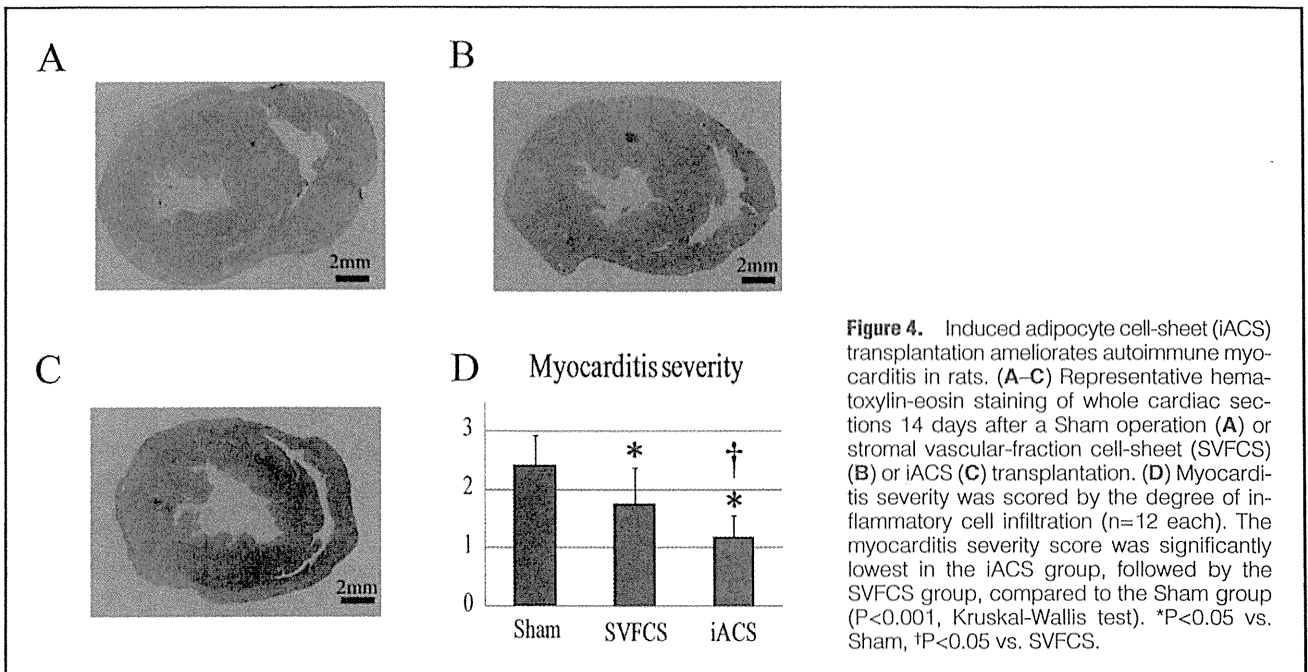


Figure 4. Induced adipocyte cell-sheet (iACS) transplantation ameliorates autoimmune myocarditis in rats. (A–C) Representative hematoxylin-eosin staining of whole cardiac sections 14 days after a Sham operation (A) or stromal vascular-fraction cell-sheet (SVFCS) (B) or iACS (C) transplantation. (D) Myocarditis severity was scored by the degree of inflammatory cell infiltration (n=12 each). The myocarditis severity score was significantly lowest in the iACS group, followed by the SVFCS group, compared to the Sham group (P<0.001, Kruskal-Wallis test). *P<0.05 vs. Sham, †P<0.05 vs. SVFCS.

each).¹⁰ Inflammatory cells with polymorphous nuclei were abundant throughout the sham-treated hearts (Figure 4A). The degree of accumulation was globally less in the iACS group, in which it was localized around the blood vessels or near the pericardial tissue, than in the other groups (Figures 4B,C). The myocarditis severity score was significantly smallest in the iACS group, followed by the SVFCS group (P=0.001 for iACS vs. SVFCS vs. Sham; Figure 4D).

The distribution of accumulated cells that regulate immune reactions, such as macrophages, T cells, and regulatory T cells, was evaluated by immunohistolabeling for CD68, CD4, and CD4/Foxp3, respectively.

The accumulation of CD68-positive macrophages and CD4-positive T cells in the myocardial interstitium was markedly and significantly lower in the iACS group than in the Sham group ([CD68: P<0.001 for iACS vs. SVFCS vs. Sham] [CD4: P<0.001 vs. iACS and SVFCS vs. Sham]) (Figures 5A,B,D). Although Foxp3/CD4-double positive regulatory T cells were not abundant in the myocardium of any group, the ratio of Foxp3-positive to CD4-positive T cells was significantly greater in the iACS and SVFCS groups than in the Sham group (P=0.006 for iACS and SVFCS vs. Sham; Figures 5C–E).

The levels of molecules that regulate immune reactions or inflammation, such as IFN γ , monocyte chemoattractant protein (MCP)1, tumor necrosis factor (TNF) α , and IL17, in the heart tissue, were significantly lower in the iACS and the SVFCS groups compared to the Sham group, as assessed by using an ELISA (Figure 5F).

Reverse LV Remodeling by iACS Transplantation in EAM Rats

Typical histological features of LV remodeling, such as myocyte hypertrophy, capillary density and collagen accumulation, were assessed in the LV of the EAM rats by using H&E staining, immunohistolabeling for CD31, and Masson-trichrome (MT) staining, respectively. On day 42, H&E staining revealed that the myocyte diameter was significantly smaller in the iACS group than in the SVFCS and Sham groups

(P<0.001 for iACS vs. SVFCS and Sham) (Figures 6A,C). However, there were no significant differences in vascular-capillary density among the 3 groups (Figure S2). MT staining of the non-inflamed area showed that the percentage of fibrosis was significantly smaller in the iACS and SVFCS groups than that in the Sham group (iACS, 4.5 \pm 2.1; SVFCS, 6.1 \pm 2.2; Sham, 21 \pm 6%; P<0.001; Figures 6B,D). MT-stained whole hearts showed a more severely enlarged LV cavity and thin LV wall in the Sham group compared with the iACS or SVFCS groups.

Quantitative real-time PCR of these samples showed that the expressions of transforming growth factor (TGF) β , metalloproteinases (MMP)2, and MMP9 were significantly lower in the iACS and SVFCS groups compared with the Sham group (Figure S3).

Preserved Cardiac Performance by iACS Transplantation in the EAM Rats

Cardiac performance after treatment was evaluated by serial echocardiography every 7 days and by cardiac catheterization on day 42. The hearts of all the groups showed gradually decreased LVEF (Figure 7A) and increased RWMI (Figure 7B) until day 56. However, the progressive changes in LVEF and RWMI were significantly least severe in the iACS group, followed by the SVFCS group, and then the Sham group (LVEF on day 56: iACS, 56.7 \pm 5.0; SVFCS, 46.9 \pm 7.2; Sham, 35.3 \pm 5.0%; P<0.001 for iACS vs. SVFCS vs. Sham). The hearts of all the groups showed a gradually decreased LV anterior wall diameter (AWD) and enlarged LV end-diastolic dimension (EDD) until day 56. Both LVAWD and LVEDD on day 42 were significantly larger and smaller, respectively, in the iACS and SVFCS groups than in the Sham group (Figures 7C,D; LVAWD: P<0.001 for iACS and SVFCS vs. Sham; LVEDD: P<0.001 for iACS and SVFCS vs. Sham). Cardiac catheterization using a conductance catheter revealed that the end-systolic pressure-volume relationship (ESPVR) was significantly greater in the iACS group than in the Sham group (P<0.001 for iACS vs. SVFCS vs. Sham; Figure 7E).

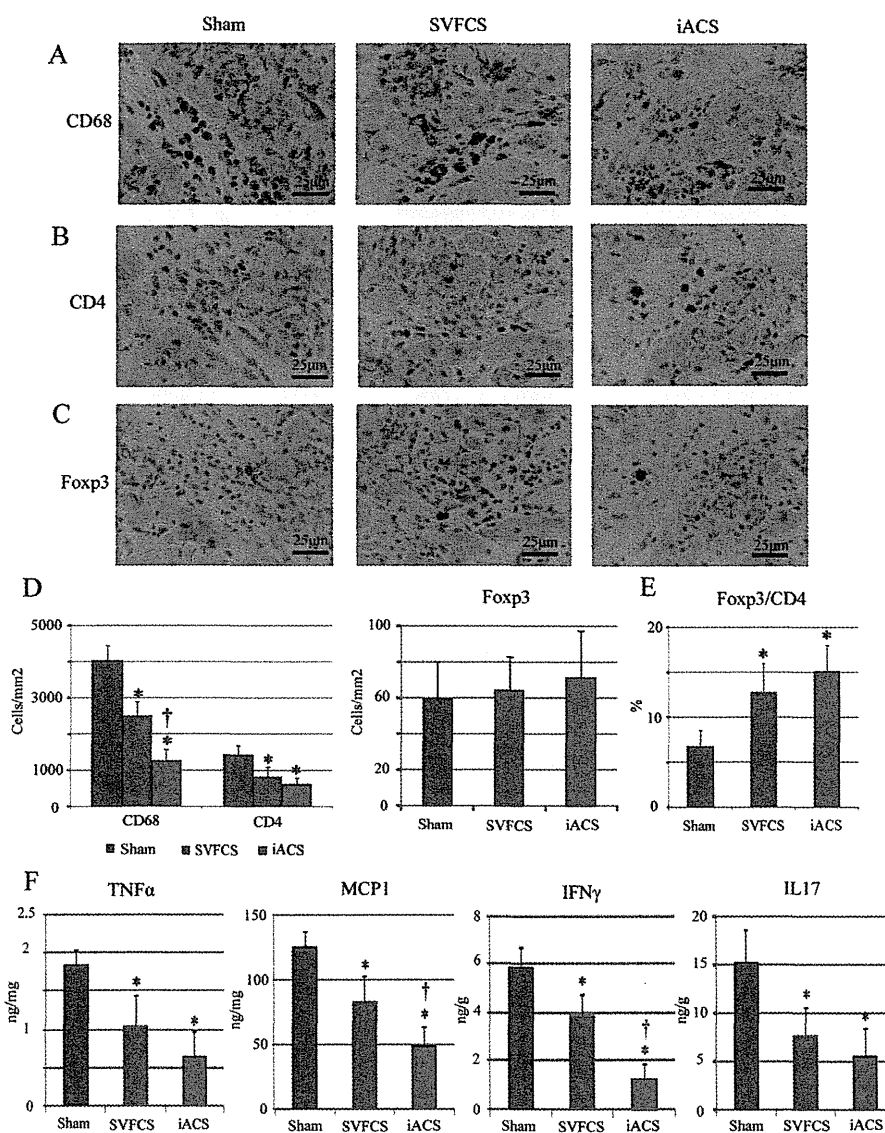


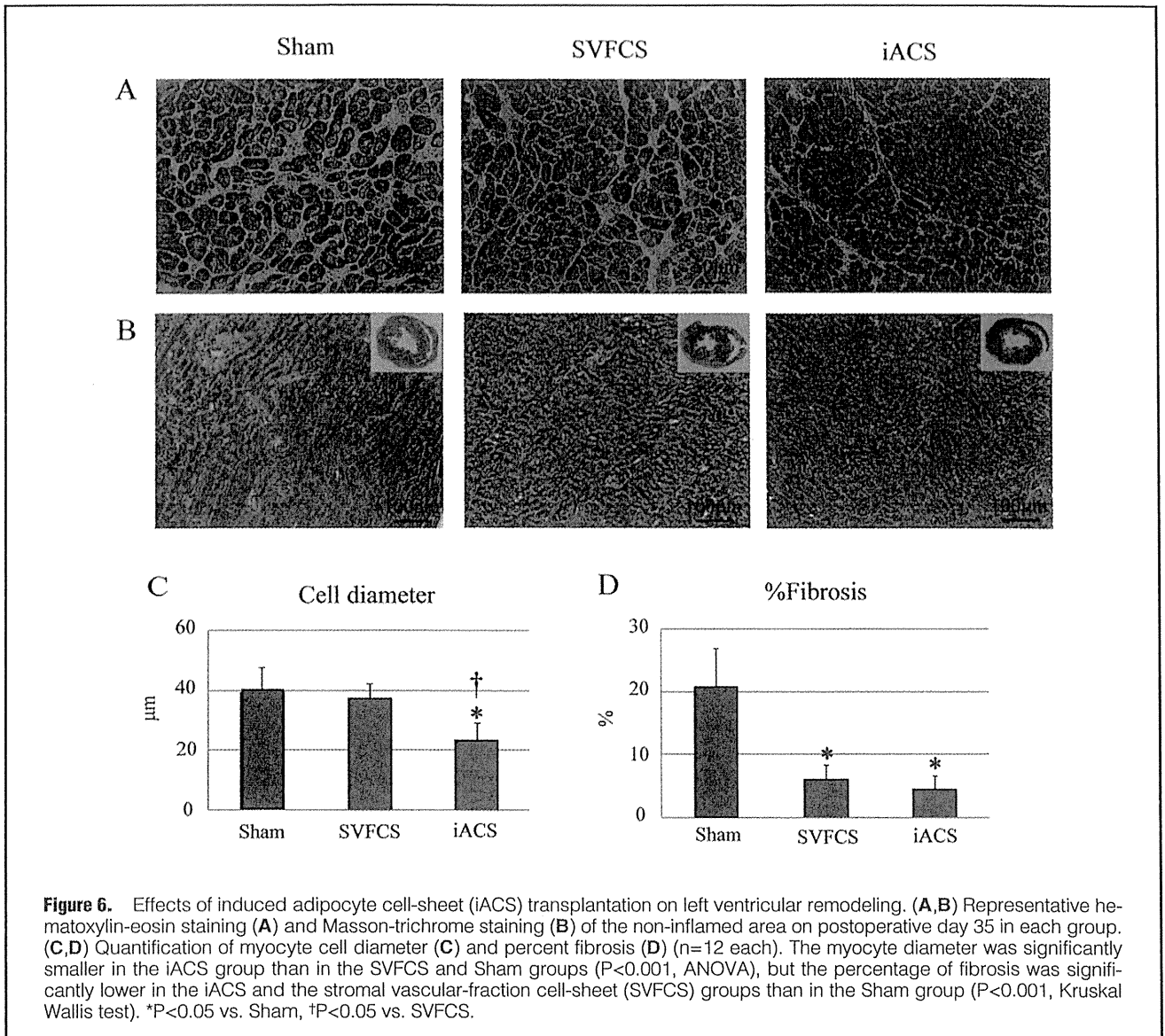
Figure 5. Induced adipocyte cell-sheet (iACS) suppressed the effector T-cell and macrophage responses, and promoted the regulatory T-cell response in experimental autoimmune myocarditis (EAM) rat heart. (A–C) Representative immunostaining for CD68 (A), CD4 (B), and Foxp3 (C) on postoperative day 14 in each group. (D) Quantification of CD68, CD4, and CD4/Foxp3-positive cells (n=12 each). CD68-positive macrophage accumulation in the myocardial interstitium was lowest in the iACS group followed by the stromal vascular-fraction cell-sheet (SVFCS) group compared to the Sham group ($P<0.001$, ANOVA). * $P<0.05$ vs. Sham, † $P<0.05$ vs. SVFCS. (E) Ratio of Foxp3-positive regulatory cells to CD4-positive T cells. * $P<0.05$ vs. Sham (n=12 each). (F) Myocardial tissues of EAM rat were homogenized and subjected to ELISA to detect tumor necrosis factor (TNF) α , monocyte chemoattractant protein (MCP)1, interleukin (IL)17, and interferon (IFN) γ (n=12 each). * $P<0.05$ vs. Sham, † $P<0.05$ vs. SVFCS.

In addition, both dP/dt max and $-dP/dt$ min were significantly greater in the iACS group than in the other groups (Table S1).

Discussion

We demonstrated here that iACS, which is generated from SVF isolated from subcutaneous fat tissues, extracellularly released a variety of cardioprotective factors including APN in vitro, and the released factors efficiently inhibited antigen-specific T-cell proliferation via the downregulation of IFN γ , IL17, and IL6 in vitro. Epicardially transplanted iACS sup-

plied greater amounts of cardioprotective factors, such as APN, HGF or VEGF, into the inflamed myocardium of EAM rat hearts for at least 35 days, compared to the SVFCS transplantation or the Sham operation. Consequently, the iACS-transplanted EAM rat hearts showed less severe inflammation, lower expression levels of inflammatory cytokines, and a greater Foxp3-positive regulatory T-cell ratio, compared to the SVFCS-transplanted or Sham-operated EAM hearts. In addition, there was less progression of histological and functional LV remodeling in the EAM hearts following the iACS transplantation than after SVFCS transplantation or the Sham op-



eration.

Fat tissue is known to play a variety of important biological and physiological roles.^{12,13} While bloated and/or degenerated fat tissues release inflammatory and atherogenic factors, intact normal fat tissues release protective factors represented by APN, which have anti-inflammatory/apoptotic/fibrotic effects on a variety of cardiac pathologies.¹²⁻¹⁴ Importantly, protective factors, including APN, have been shown to be released by mature adipocytes, but not by undifferentiated ones such as SVF cells.⁹ Because the cell culture of freshly isolated mature adipocytes and cell-sheet generation from these cells are technically difficult, we generated cell sheets containing mature adipocytes by inducing the cells in SVFCS to differentiate in vitro. We confirmed that both the iACS and SVFCS released little inflammation-related or atherogenic adipokines in vitro. In contrast, differentiated iACS but not SVFCS could secrete a large amount of APN.

Although the lifespan of adipocytes is generally shorter than that of SVF cells, SVF cells are known to appropriately and autonomously differentiate into adipocytes in vivo in adipose

tissues in response to increased adipocyte cell death. Considering this reciprocal regulation between the 2 cell types, we ascertained that a minimum, rather than maximum, induction of differentiation might allow the iACS to provide APN to the host myocardium for a long time. In fact, iACS contained a certain amount of undifferentiated SVF cells before transplantation. While iACS supplied significantly more APN to EAM hearts than did SVFCS, the APN level in the inflamed myocardium was not different between the SVFCS-transplanted and Sham-operated hearts, suggesting that SVFCS did not release substantial APN after its transplantation into the heart. This contrary effect that SVF cells could differentiate into mature adipocytes in vitro, but not in vivo, could be explained by the different conditions for the differentiation from SVF cells to mature adipocytes. The appropriate induction of differentiation to iACS in vitro might have maintained the normal capacity of the adipocytes and/or SVF cells in the sheet to release abundant APN or other protective factors after transplantation, thereby eliciting the substantial therapeutic effects noted in this study.

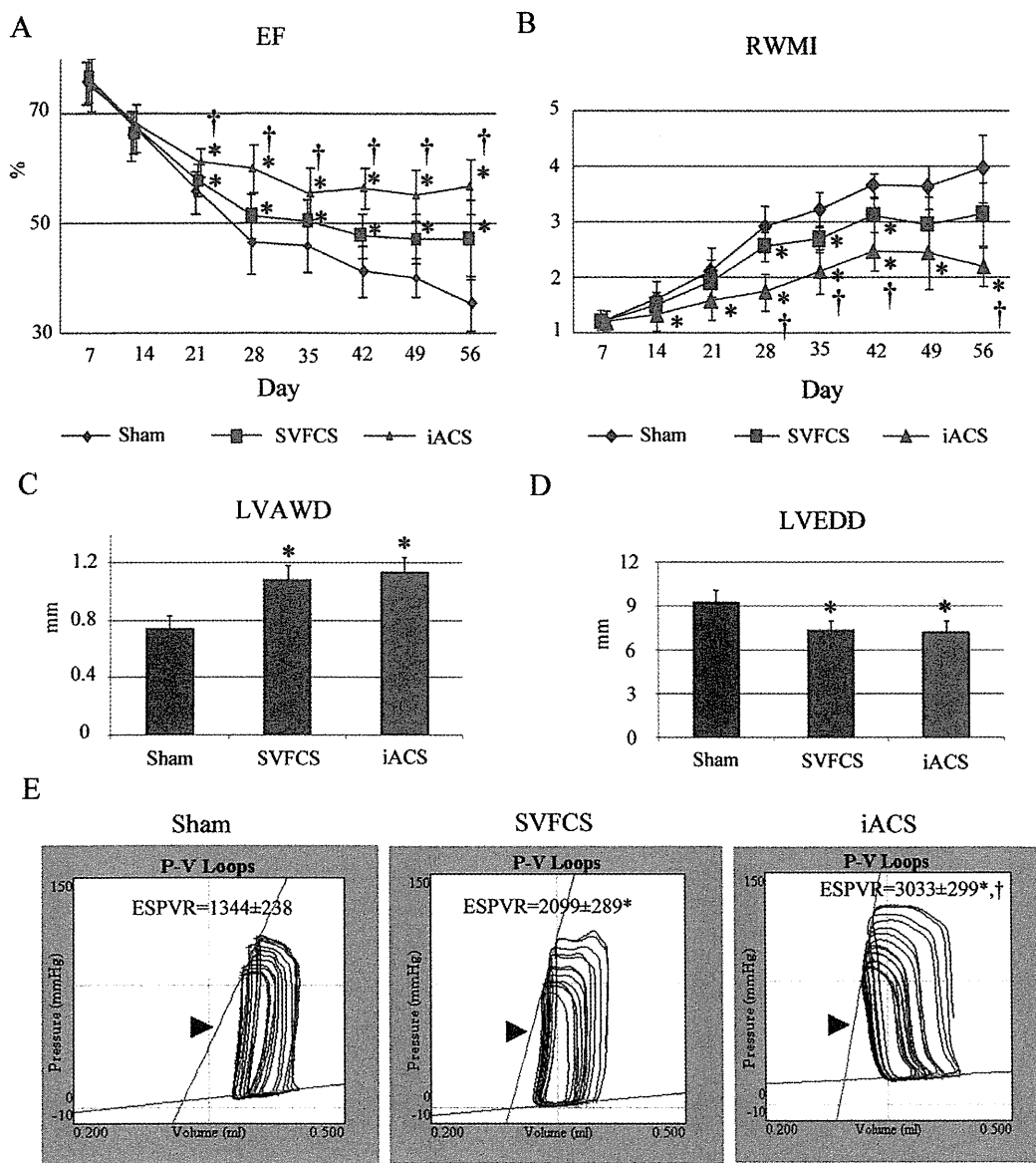


Figure 7. Cardiac structure and function after induced adipocyte cell-sheet (iACS) transplantation. **(A,B)** Serial echocardiographic parameters **(A, ejection fraction [EF], B, regional wall motion index [RWMI])** in each group (day 7–day 42, n=12 each; day 49–day 56, n=6 each). The left ventricular (LV) EF was greatest in the iACS group, followed by the stromal vascular-fraction cell-sheet (SVFCS) group, then the Sham group (P<0.001, ANOVA). *P<0.05 vs. Sham, †P<0.05 vs. SVFCS. **(C,D)** LV anterior wall diameter (LVAWD) **(C)** and end-diastolic diameter (LVEDD) **(D)** on day 42 (n=12 each). LVEDD on day 42 was significantly lower in the iACS and SVFCS groups than in the Sham group (P<0.001, Kruskal-Wallis test). *P<0.05 vs. Sham. **(E)** Representative pressure-volume (P-V) loops on day 42 from each group (n=7 in each). Slopes indicate the end-systolic P-V relationship (ESPVR) (arrows). Representative P-V loops during inferior vena cava occlusion showed that the ESPVR was significantly greater in the iACS group than in the other groups (P<0.001, ANOVA). *P<0.05 vs. Sham, †P<0.05 vs. SVFCS.

The transplantation of either SVFCS or iACS resulted in positive pathological and functional effects on the EAM hearts in this study, although the impact was greater following iACS transplantation. The findings indicate that APN, which was more substantially increased in the iACS-transplanted hearts than in the SVFCS-transplanted ones, was a key factor accounting for the difference between the iACS and SVFCS treatments.⁷ HGF and/or VEGF, which were increased in both

the iACS and the SVFCS groups, have also been suggested to elicit therapeutic effects.⁸

Importantly, following iACS transplantation, both APN and HGF were present near CD4-positive effector T cells, which are known to express APN and HGF receptors,^{7,8} suggesting that the upregulated APN and HGF might inhibit the accumulation of effector T cells and macrophages, and promote the accumulation of Foxp3 regulatory T cells, consequently at-

tenuating inflammation in the EAM hearts.

Treatment with ARB or PPAR γ increases the circulating APN concentration in humans,¹³ although these treatments are unlikely to deliver APN efficiently enough to the severely inflamed myocardium to be clinically relevant. Consistent with our results, previous reports demonstrated that the viral gene delivery of APN or HGF endogenously elevates its concentration in autoimmune myocarditis tissue, leading to immunomodulatory effects and the reversal of LV remodeling.^{7,8} In contrast to the *in vivo* viral transfection method, our cell-sheet-based delivery system eliminates concerns related to the use of plasmid vectors and of needle injection into the host myocardium, and more efficiently delivers multiple cardioprotective factors over the long term.^{9,15} After iACS implantation, the expression of cardioprotective factors (APN, HGF and VEGF) in the myocarditis tissues increased significantly, peaking at postoperative day 14, followed by stable and high expression through postoperative day 35. This prolonged and balanced delivery of cardioprotective factors might be more efficient and practical for clinical use than the one-time administration of a single reagent. Moreover, while the transplanted cells and their producing cytokines existed only in the epicardium, functional and pathological recovery by the iACS therapy was detected both in the inflamed and non-inflamed tissues, suggesting that the major therapeutic mechanisms in this study are not direct effects by transplanted cells but paracrine effects by host cardiac cells. The heart is generally formed in contractile myocardium, endocardium and epicardium, and the epicardium is thought to have a rich cardiac progenitor cell niche and to play an important role in cardiac repair.¹⁶

Notably, it has been shown that cell-sheet implantation into the epicardium induces the expression of multiple cardioprotective factors in the heart, and activates host epicardial cells crucial for cardiac repair. Therefore, these therapeutic effects in the study might be associated with the cell-sheet method. We believe that this “cross-talk” between the transplanted cells and the native myocardium activates and/or inhibits multiple pathways, leading to beneficial effects, and therefore that the cell-sheet method is a rational drug-delivery system for cardiac pathologies.

The T-cell-related immune modulatory effects were different between the EAM hearts treated with iACS vs. SVFCS transplantation in this study. While the level of Th1-producing IFN γ in the inflamed area of the heart on day 21 was lower in the iACS group than the SVFCS group, the level of Th17-produced IL17 was not significantly different between them. In addition, regulatory T cells accumulated prominently and to a similar degree in both the iACS and SVFCS groups. Nonetheless, the acute myocarditis severity on day 21 was significantly less after iACS implantation than after SVFCS implantation. The functional assessment also showed that the RWMI increase from day 7 to day 28 of the acute myocarditis phase was less in rats receiving iACS implantation than SVFCS implantation. Thus, the acute myocarditis severity on day 21 might be mainly associated with the Th1-mediated autoimmune response. In contrast, iACS implantation significantly elevated the level of APN in the myocarditis tissue, compared with SVFCS implantation. A T-cell proliferation assay showed that the addition of iACS supernatant, which contained APN and HGF, significantly decreased the level of Th1-producing IFN γ , compared with the addition of recombinant HGF alone. These findings indicated that the greater immunosuppressive effects of iACS implantation on effector Th1 cells compared with SVFCS implantation might be associated with the synergistic paracrine effects of APN and

HGF released by the implanted iACS.

Regulatory T cells and effector Th17 cells might be reciprocally regulated in various autoimmune diseases.³ In our study, some reciprocity between the number of accumulated Foxp3 regulatory T cells and the amount of IL17-producing Th17 in the myocarditis tissues was observed among the groups. ELISA analysis of the myocarditis tissues on day 21 showed that the iACS and SVFCS implantation similarly suppressed Th17 cells and activated the Foxp3 regulatory T cells. Recently, Baldeviano et al. reported that Th17-produced IL17 was dispensable for the severity of the acute myocarditis, but essential for the progression of cardiomyopathy.³ Consistent with this, we found that the cardiac fibrosis related to LV remodeling in the chronic cardiomyopathy phase was similarly attenuated in the iACS and SVFCS implantation-treated rats via the suppression of profibrotic factors: TGF β , MMP2, and MMP9. Thus, this inhibition of morphological deterioration might be associated with the suppression of the Th17-mediated autoimmune response and the induction of immune tolerance. In accordance with this scenario, morphological LV remodeling, such as LV dilatation and LV thinness, on day 42 was similarly suppressed in the groups receiving iACS and SVFCS implantation. In addition, the assessment of RWMI showed that the LV functional deterioration from day 28 to day 56 of the chronic cardiomyopathy phase was similarly suppressed in the rats receiving iACSs and SVFCSs, compared with the Sham operation. However, the cardiac hypertrophy on day 42 was attenuated only in the group receiving the iACSs. Several lines of evidence have indicated that APN directly affects injured myocytes via its receptor, eliciting anti-hypertrophic effects in a pressure-overload hypertrophic model.^{13,17} Thus, the significant suppression of hypertrophy in iACS implantation-treated rats might have resulted from direct and synergistic effects of APN and HGF on the injured myocytes, and not from indirect immune modulatory effects via effector Th17 cells.

This study showed that iACS implantation had beneficial immunologic, pathologic, and functional effects on the heart of rats with autoimmune-associated myocarditis. However, in the clinical setting, fulminant myocarditis is etiologically highly heterogeneous, and thus, the autoimmune activity associated with it varies. The effectiveness of the iACS treatment shown in this study is therefore not directly translatable to the clinical situation. The investigation of T-cell activity by cardiac biopsy or circulating blood samples from patients with fulminant myocarditis might be useful for identifying responders or determining whether iACS treatment is indicated.

Normally, human myocarditis has a sudden onset and it has been known that it often follows a rapidly deteriorating course, leading to severe cardiac dysfunction. It has been reported that early diagnosis and subsequent treatment for fulminant myocarditis might be essential in clinical practice.¹ Therefore, methods need to be developed for promptly generating autologous iACS to maximize its therapeutic effects. The use of allogeneic iACS might be an option for clinical applications. Although there are immunologic concerns associated with the use of allogeneic iACS, this study suggested that iACS treatment upregulated APN and HGF, which attenuated the immunological response by inhibiting macrophages and activating regulatory T cells. Moreover, APN can limit allograft rejection by suppressing the expression of local cytokine/chemokine ligands that mediate inflammation and immune-cell recruitment.¹⁸ Thus, the need for immunosuppressive medications might be minimal for allogeneic iACS treatment, although further study is needed.